*Int. J. Electrochem. Sci.*, 10 **(2015)** 9475 - 9487

International Journal of
ELECTROCHEMICAL
SCIENCE
www.electrochemsci.org

*Short Communication*

# Covalently Functionalized Graphene Oxide – Characterization and Its Electrochemical Performance

*Safina Iram Javed, Zakir Hussain*[*]

School of Chemical and Materials Engineering (SCME), National University of Sciences & Technology (NUST), Sector H-12, 44000 Islamabad, Pakistan
Tel.: 0092 51 9085 5205; Fax. 0092 51 9085 5002
[*]E-mail: zakir.hussain@scme.nust.edu.pk

*Received:* 6 August 2015 / *Accepted:* 24 August 2015 / *Published:* 30 September 2015

In this study, graphene oxide (GO) was synthesized through chemical ex-foliation process from graphite flakes. GO was further covalently functionalized with Levofloxacin (LOF) by Steglich esterification reaction. Herein, we describe a method for the chemical functionalization and in-situ reduction of GO using LOF as a reducing agent. GO was reduced and remained well dispersed after reduction in the solution even after 6 months. The functionalized and reduced GO was characterized through range of analytical techniques. Functionalized GO was further used as a supercapacitor (SC) electrode material and its electrochemical behavior was compared with GO and reported. Capacitance of functionalized GO was found to be four times the capacitance of GO, indicating significantly enhanced electrochemical performance of functionalized GO as compared to pure GO.

**Keywords:** Graphene oxide; Esterification; Functionalization; Reduction; Supercapacitor

## 1. INTRODUCTION

Graphene, flat single layer of carbon atoms which is packed into 2D honeycomb lattice, is a building block for all graphitic materials. It can be transformed in the form of 0D fullerenes, 1D nanotubes or 3D graphite [1]. Research on graphene has revealed huge theoretical and practical advantages such as large surface area, excellent conductivity, very good capacitance, and relatively low production cost [2]. Due to its excellent mechanical [1], electrical [3], thermal [4], and transport properties [5] it has found many potential applications in sensors, nano-composites, supercapacitors and hydrogen storage.

Graphene of highest quality can be produced by mechanically exfoliating crystalline graphite [6]. However, the amount of graphene produced by this method is small and is sufficient for research purposes only [2]. Chemical oxidation of graphite into graphene oxide (GO) [7] then its subsequent

reduction by hydrazine hydrate [8] is an alternate method that has been used widely for the mass production of graphene.

During the reduction process hydrophilicity of water dispersed graphene oxide sheets decreases which results in the agglomeration and precipitation of graphene sheets [9]. Moreover, hydrazine hydrate which is employed as reducing agent, is explosive and poisonous [10]. Therefore, a new approach is required for the stable conversion of GO into graphene sheets. Aggregation of graphene sheets during the reduction process can be inhibited by covalent or non covalent functionalization so that intrinsic properties of graphene can be retained [11]. Since reduction of GO dispersions without any stabilizing agent results in the aggregation of graphene sheets. Thus reduction reaction is carried out after the covalent or non-covalent functionalization of GO sheets [12]. Functionalization can be accomplished in two ways. Either to covalently attach external atoms directly with the carbon of graphene that leads to the tuning of electronic structure and formation of defect sites or to covalently couple the native functional group of GO with the guest functional group. Along with diverse electrical properties compared to undoped graphene, increased thermal stability and mechanical strength is also achieved as a result of functionalization [13].

In our present study, LOF was covalently coupled on the graphene surface which leads to the simultaneous functionalization and reduction of GO sheets. The electrochemical charge storage behavior of the supercapacitor electrode with functionalized graphene has been studied in an aqueous medium. Cyclic voltammetery measurements indicated successful reduction of GO films [14]. This is the first time we are reporting the reduction of GO through LOF. Further, no one has reported the application of *f*-(LOF)GO as a supercapacitor electrode with enhanced capacitance compared to the GO as supercapacitor electrode.

## 2. EXPERIMENTAL

### *2.1. Materials*

Flake graphite (500 mesh, Sigma Aldrich), (S)-9-fuoro-2,3-dihydro-3-methyl-10-(4-methyl-1-piperazinyl)-7-oxo-7H-pyrido[1,2,3-de]-1,4-benzoxazine-6-carboxylic acid(LOF), *N*,*N*'-dicyclohexylcarbodiimide (DCC, Sigma Aldrich), 4-dimethyl-amino-pyridine (DMAP, Sigma Aldrich), sulphuric acid (98%,1.84 $gmol^{-1}$), phosphoric acid (85%,1.68 $gmol^{-1}$), hydrogen peroxide (30%,1.11$gmol^{-1}$), potassium permanganate, hydrochloric acid (37%,1.2$gmol^{-1}$), acetone, IPA (Isopropanol), dimethyl sulfoxide (DMSO), sodium sulphate and deionized water. All the chemicals were of analytical grade and these were used without any further refinement.

*2.2. Synthesis of Graphene Oxide*

A simple room-temperature preparation technique, reported for the production of large-area GO, was used for the synthesis of GO [7]**.** In a typical synthesis, graphite flakes (1.0g) were added under magnetic stirring into 130 mL of pre-mixed acids ($H_2SO_4$ and $H_3PO_4$; 9:1). After stirring for 5 minutes, $KMnO_4$ (3.0g) was added very slowly, into the mixture during magnetic stirring (400 rpm) resulting into an exothermic reaction (temperature raised 50$^o$C). Stirring continued for another three days at room temperature and subsequently, 5ml of $H_2O_2$ (30%) was added to the mixture, resulting into the formation of vigorous bubbles and dark brown colour of the mixture turned into bright yellow. After stirring for further 5 minutes, the mixture was washed repeatedly through centrifugation at 4000 rpm with 1.0M HCl and DI water until its pH was 7.0, resulting into the ex-foliation of graphite oxide and formation of GO gel.

*2.3. Co valent Functionalization of GO with LOF*

LOF was covalently coupled onto the surface of graphene oxide through Steglich esterification with the help of DCC and DMAP as catalysts [15]. The functionalization process is sketched in Figure 1. In this particular reaction, 12ml GO gel (1.5mg/mL) was centrifuged at 4000rpm for 2hrs for water decantation. Then GO (18.0mg) was dispersed in 10 mL of dimethyl sulfoxide (DMSO) and the mixture was sonicated (200W) for 30 min for exfoliation and formation of clear suspension of GO in DMSO.

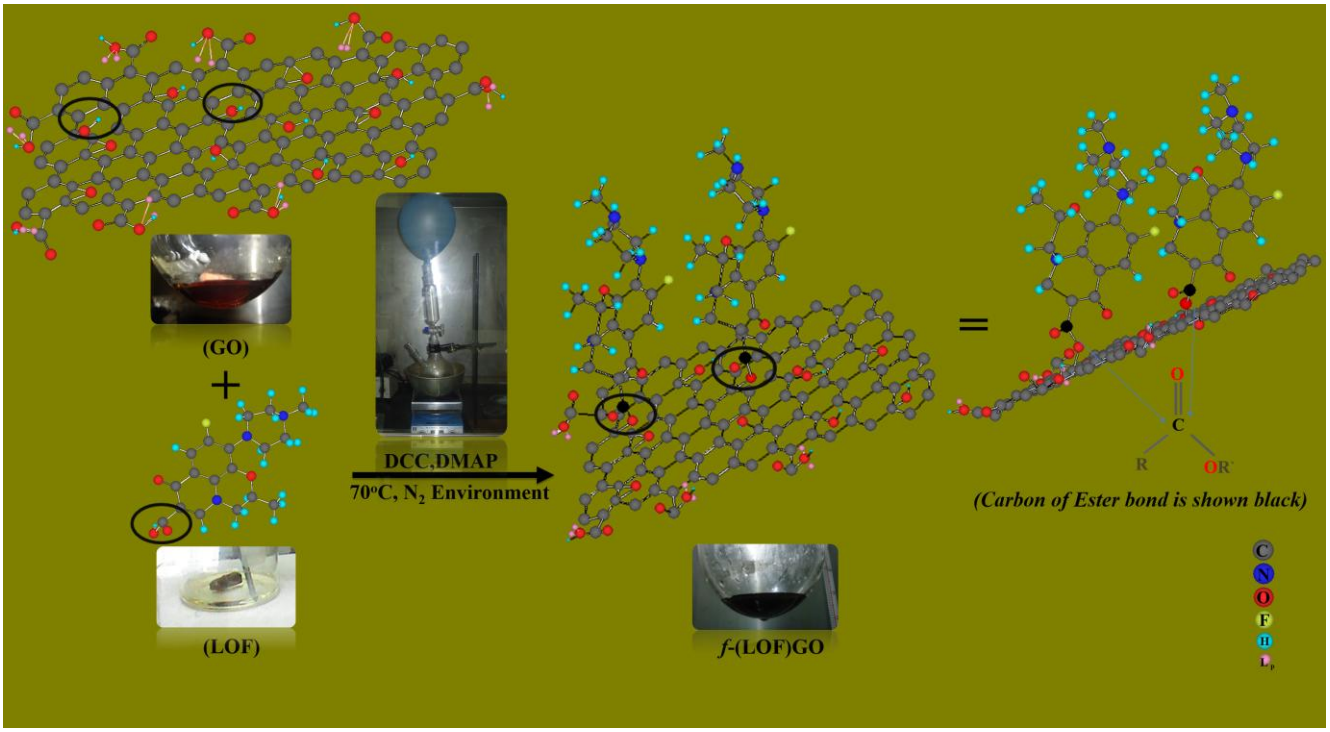


**Figure 1.** Illustration of the covalent-functionalization of GO.

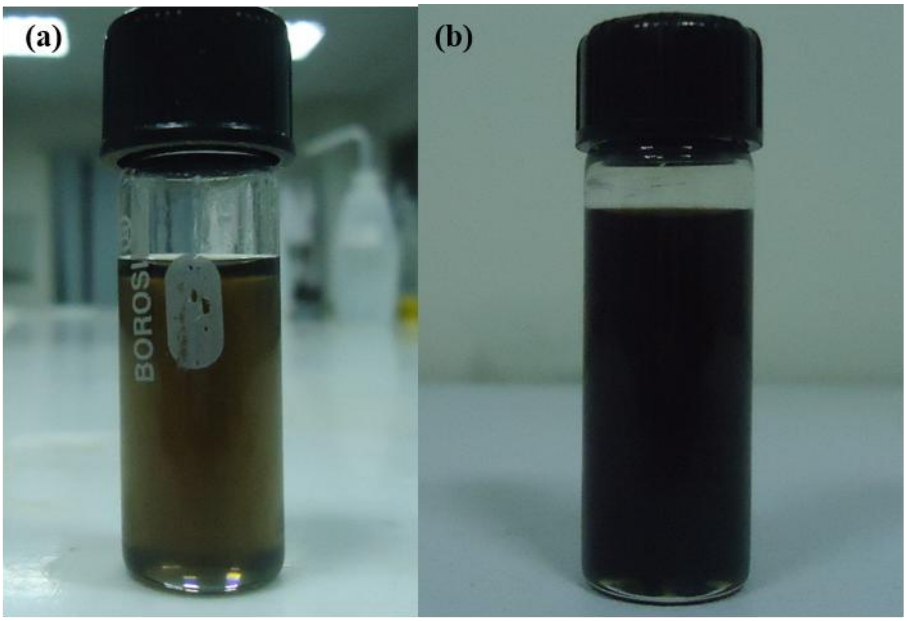


**Figure 2.** Digital photographs of dispersions of GO before and after functionalization and in-situ reduction (a) GO dispersed in DMSO (b) *f*-(LOF) GO in DMSO

Homogenous solution of LOF (25 mM) was prepared separately by stirring 180mg of LOF in 20 ml DMSO for 30min. at room temperature under an inert environment of $N_2$. Subsequently, LOF/DMSO solution and GO/DMSO suspension were mixed under stirring (300 rpm) at room temperature in an inert environment. After about 30 min stirring, temperature of the mixture was raised to 70 $^oC$ and magnetic stirring was continued for next 24hrs. DCC (832.0mg) and DMAP (61.0mg) were added in the mixture and stirring continued for further 28 hrs at 70 $^oC$. The reaction mixture was cooled to room temperature and stirring was continued for another 36 hrs. Subsequently, 40 mL of acetone was added to the mixture and the precipitate was re-suspended in DMSO and centrifuged at 4000 rpm twice for the removal of un-reacted LOF. To remove the solvent, the solution was dried under high vacuum ($10^{-6}$) for 24hrs and the dried functionalized graphene oxide was obtained in the powder form referred to as *f*-(LOF)GO. The dried product was then used for the characterization purposes. Figure 2 shows the optical appearances of pristine as well as chemically functionalized GO. In these images, color of the solution turned from brown to black after the functionalization, indicating the reduction of the GO as reported by others [14, 16, 17].

### *2.4. Preparation of electrodes for electrochemical analysis*

GO and *f*-(LOF)GO were used as active materials for the electrochemical analysis. Aluminum foil (Al) was used as a current collector and substrate for electrode in an electrochemical cell. Al-foil was cleaned with IPA and acetone and subsequently rinsed with DI water.

Following the procedure, *f*-(LOF)GO was drop casted onto the Al-foil in a petri dish and dried in an oven at 50 $^oC$ for 3hrs. Rectangular shape electrodes (50x25$mm^2$) were cut to check the electrochemical response of the active material for supercapacitor applications [18]. These coated Al-

foils were sandwiched by a filter paper that was soaked in 1M sodium sulphate solution. The sandwiched foils were clamped and secured with a pair of glass slides and clippers.

### *2.5. Characterization:*

Oxidation of graphite and covalent coupling of LOF with graphene oxide was analyzed through (FT-IR) spectra that were recorded between 4000 and 400 $cm^{-1}$with 4 $cm^{-1}$ resolution on a PerkinElmer spectrum 100 (FT-IR spectrometer), using a KBr disk method. The X-ray diffraction (XRD) pattern was obtained on a STOE Powder X-ray diffractometer θ-θ (operating voltage 40 kV and current 40mA) utilizing a scanning rate of 0.5° $min^{-1}$ ranging from 5° to 80° (2θ) with Cu Kα radiation (λ = 1.5418 Å). Ultraviolet-visible (UV-Vis) spectra were recorded using a WPA Biowave II spectrophotometer (Biochrom, Cambridge, UK). Microstructure and surface morphology of the prepared GO and *f*-(LOF)GO were studied using Nano NOVA FE-SEM at an accelerating voltage of 15kV with magnification range 20X to 5000X. Energy dispersive X-ray (EDX) measurements were performed between 0 and 20 kV. Optical imaging of the materials was performed using Olympus digital camera. The electrochemical behavior of the supercapacitor was characterized through cyclic voltammetery using a multipotentiostat/galvanostat (BioLogic VSP system). Cyclic voltammograms were recorded between –0.1mV and +1.0V at scan rate 50 mV and 100 mV. All experiments were conducted at room temperature (~298 K). CV-measurements, of the electrochemical cell fabricated with GO and *f*-(LOF)GO, were conducted in 1M $Na_2SO_4$ solution in a two electrode configuration test cell.

## 3. RESULTS AND DISCUSSION

### *3.1. UV-Vis Spectroscopy*

UV-vis spectroscopy was used to examine the degree of oxidation for the GO and functionalized GO samples. $\lambda_{max}$ of the UV-Vis spectrum is used to reveal the degree of residual conjugation in both the pristine and functionalized GO. A higher $\lambda_{max}$ in the spectrum represents that less energy has been used for the electronic transition which is an indication of the restoration of conjugation [19]. The spectrum in Figure 3(a) shows absorption peak of GO at 230 nm. The $\pi \rightarrow \pi^*$ transition of C-C , C=C bonds present in the $sp^2$ hybrid areas of GO is the main cause for the appearance of this peak, as already described in the literature [20]. UV-Vis spectrum of pure LOF contains peak at 292nm associated with the $\lambda_{max}$ of LOF [21]. In figure 3(b) the UV-Vis spectrum of the coupled product shows that the peak of GO has been red shifted to 268nm which is attributed to the reduction of GO and to the n-$\pi^*$ transition of C-O bonds as reported previously [22]. The 299nm peak may corresponds to the $\lambda_{max}$ of LOF with a bathochromic shift (7nm) attributed to the aromatic interaction between LOF and RGO similar to the red shift in pyrene's intrinsic absorption peak [23]. and the observation of bathochromic shift in its Soret band of the porphyrin [24].

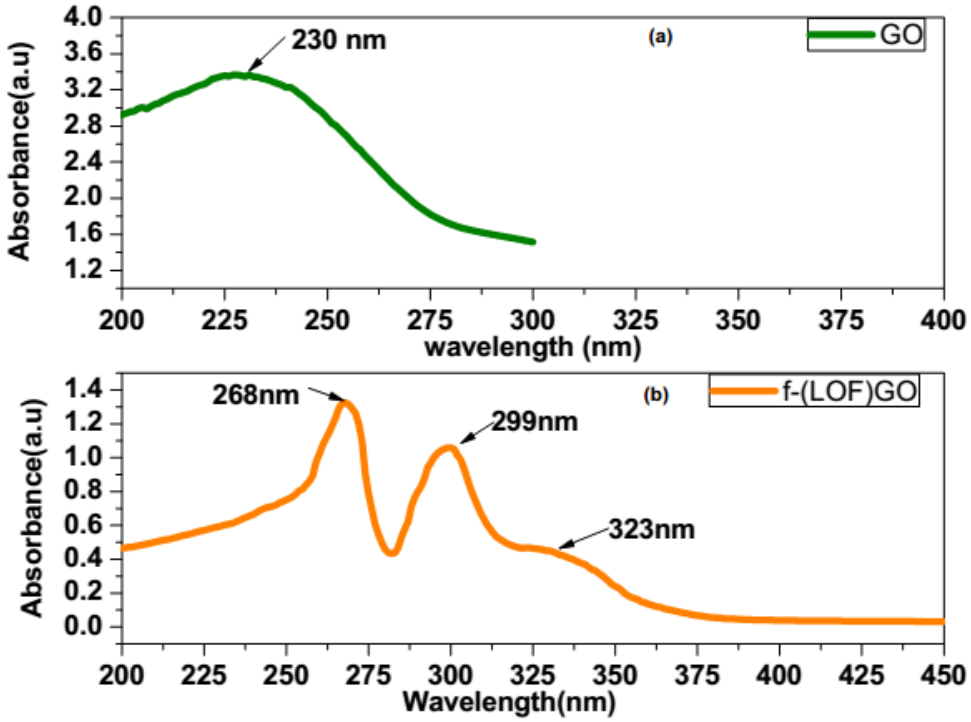


**Figure 3.** The UV-Vis spectra of (a) GO and (b) *f*-(LOF)GO

*3.2. FTIR Spectroscopy*

FTIR is used for the semi-quantitative analysis of chemically functionalized GO due to the sensitivity of IR to the creation as well as change of chemical bonds [13]. In the IR-spectrum of graphite, the absorption bands at 3433 cm-$^{1}$ was known to be the O-H stretching vibrations; the peak located at 1632 cm$^{-1}$could be assigned to the presence of skeletal vibration of C=C from sp$^{2}$ CC bonds [25]. After the oxidation reaction, the FT-IR spectra of GO apparently changed compared to that of graphite. The IR spectrum of GO shows the strong C=O stretching band at 1727 cm$^{-1}$ [26]. The peak near 3398 cm$^{-1}$ is due to the O-H stretching vibrations and the peak at 1626 cm$^{-1}$ corresponds to the sp$^{2}$ character of C=C [27].The peaks at 1262cm$^{-1}$ and 1405cm$^{-1}$ are due to the epoxy C-O and C-OH vibrations respectively [25, 28]. FT-IR results indicated that oxygen-containing functional groups were established successfully onto the surface of graphite during the oxidation reaction. Figure 4(b) shows the IR spectrum of LOF with major peaks at about 559, 581, 650,745.1, 802, 838.67, 873, 929, 977, 1027, 1084, 1193, 1242, 1292, 1305.0, 1333, 1517,1621, 1727, 2797, 3080 and 3262 cm$^{-1}$ etc. as reported previously [29]. In Figure 4(c), the characteristic carboxyl C=O peak of LOF diminished and also intensity of the broad band corresponding to the O-H stretching vibrations is significantly reduced. Two new intense peaks appeared at 2853 cm$^{-1}$ and 2923 cm$^{-1}$ that represents symmetric and antisymmetric =$CH_2$ vibrations of graphene [30]. Moreover the peaks at 1650 cm$^{-1}$ and 1207cm$^{-1}$ represents the formation of ester, indicating successful coupling of the LOF on the surface of GO through esterification reaction.

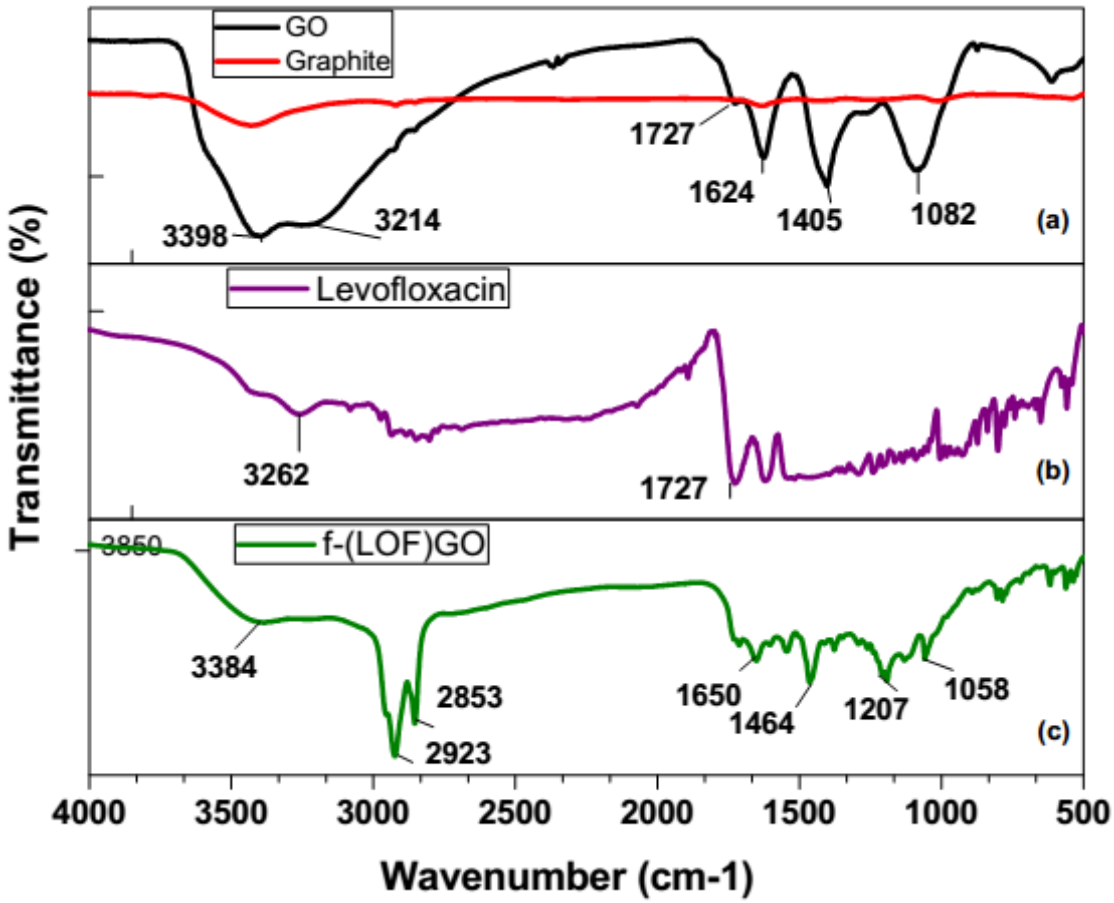


**Figure 4.** FTIR spectrum of (a) Graphite and GO, (b) LOF, (c) *f*-(LOF) GO

*3.3. Microscopic Analysis*

Scanning electron microscope (SEM) image in Figure 5(a), shows that the lateral dimension of GO varies between 1-10µm. The light gray areas found on the substrate represent few layered GO sheets and dark gray areas represent multi-layered GO sheets. These micro-graphs showed very good exfoliation of GO sheets at the given conc. Figure 5 (b) shows the SEM image of the functionalized *f*-(LOF)GO separated from the solvent by filtration and vacuum drying. The cross-sectional image, as shown in Figure 5(c), displays the layer-by-layer stacking of the functionalized graphene sheets. Thickness of the coating was 6.3µm. The cross-section of thin layer of *f*-(LOF) GO suggests that upon drying at 50$^{o}$C, DMSO-dispersed graphene sheets accumulated into layer-by-layer pattern. To see the effect of heat on the morphology of the *f*-(LOF) GO coating it was heated at 200 $^{0}$C in a glove box under inert atmosphere and then its micrograph was taken in the SEM. The image 5(d) shows that upon heating, coating of the coupled product from Al-foil peeled off and several cracks developed in the deposited film. This phenomenon explains the decrease in current (depicted in CV graphs) of the electrodes due to the loss in electrical contact between current collector (Al-foil) and the supercapacitive layer of functionalized GO. Figure 5(e-f) shows the micro-image of functionalized graphene extracted from the solvent with vacuum filteration. Table 1 shows the information obtained from the EDX spectrum showing the elemental composition of the coupled product which shows the

presence of C, O, N and S. C and O are contributed by RGO while N indicated the coupling of LOF. C/O ratio in the EDX analysis indicates successful formation of the nano-hybrid as reported by others [14, 31]. The presence of sulfur is supposed to arise from the sulfuric acid used in the synthesis method for the preparation of graphene oxide [32].

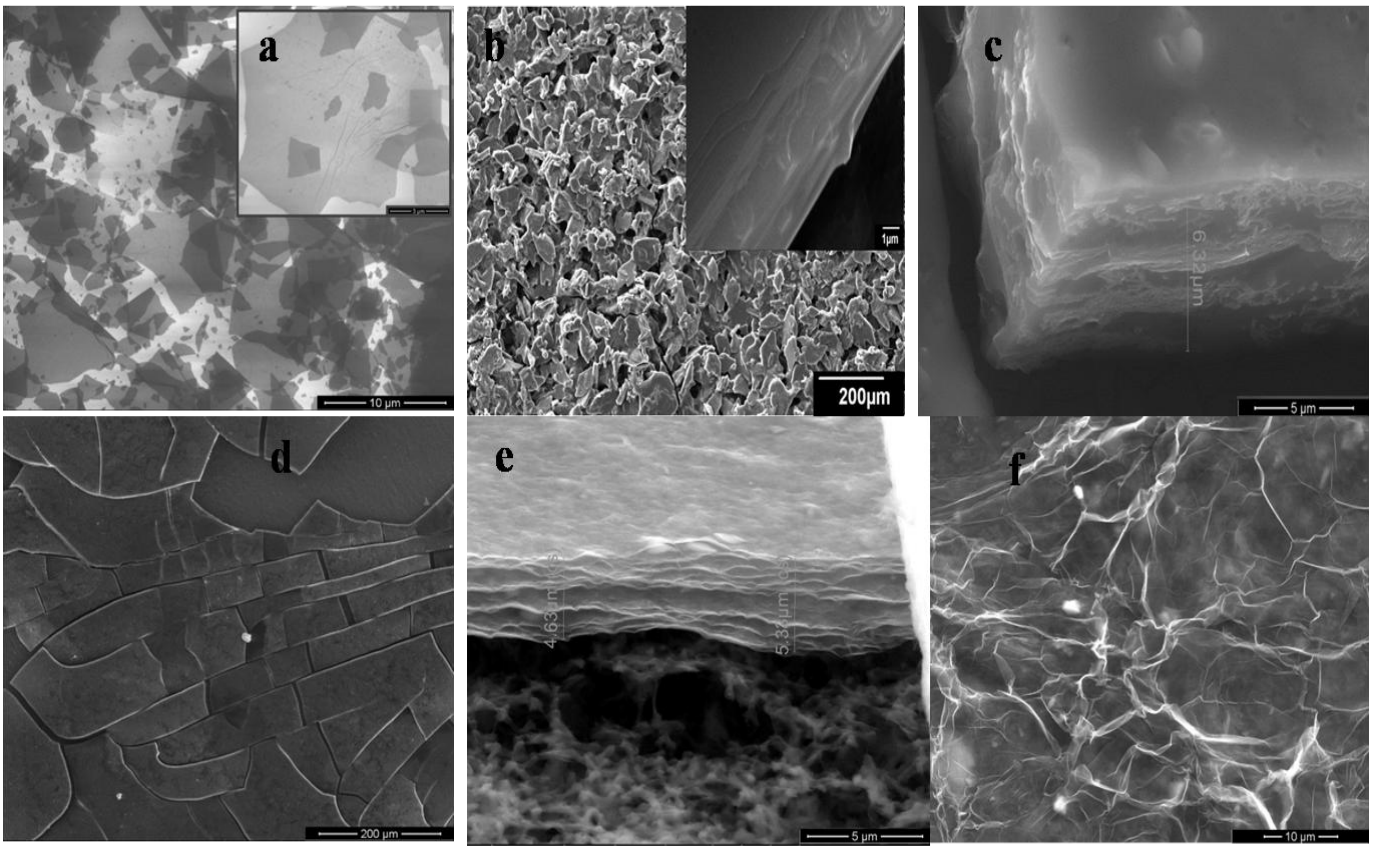


**Figure 5.** FESEM images of (a) Exfoliated GO coated on Si substrate (b) vacuum dried *f*-(LOF)GO in powder form (c) *f*-(LOF)GO coating on Al-foil (d) *f*-(LOF)GO coated Al-foil heated at 200$^{o}$C (e) cross-sectional view of vacuum filtered *f*-(LOF)GO (f) Topography image of *f*-(LOF)GO in (e).

**Table 1.** Elemental analysis (EDX profile) of the functionalized graphene

| **ZAF Method Standardless Quantitative Analysis (Fitting Coefficient : 0.9101)** | | | | |
|---|---|---|---|---|
| **Element** | **(keV)** | **Mass %** | **Error %** | **Atom %** |
| C | 0.277 | 37.01 | 0.35 | 41.58 |
| N | 0.392 | 44.90 | 5.80 | 43,26 |
| O | 0.525 | 17.85 | 5.79 | 15.06 |
| S | 2.307 | 0.24 | 0.66 | 0.10 |
| Total | | 100.00 | | 100.00 |

*3.4. Structural analysis*

XRD pattern in Figure 6 (a) shows a distinct diffraction peak (001) of GO at 10.05°. The interlayer spacing value "*d*" for GO is 0.87nm which has been calculated from the following Bragg`s law [33].

$$2dsin\theta = \lambda$$

**Table 2.** GO properties deduced from XRD data file by using X'Pert HighScore software

| Pos. [°2Th.] | Height [cts] | d-spacing [Å] | FWHM [°2Th.] | Tip width [°2Th.] | Rel. Int. [%] |
|---|---|---|---|---|---|
| 10.0502 | 2692.42 | 8.79417 | 0.4320 | 0.5184 | 100.00 |

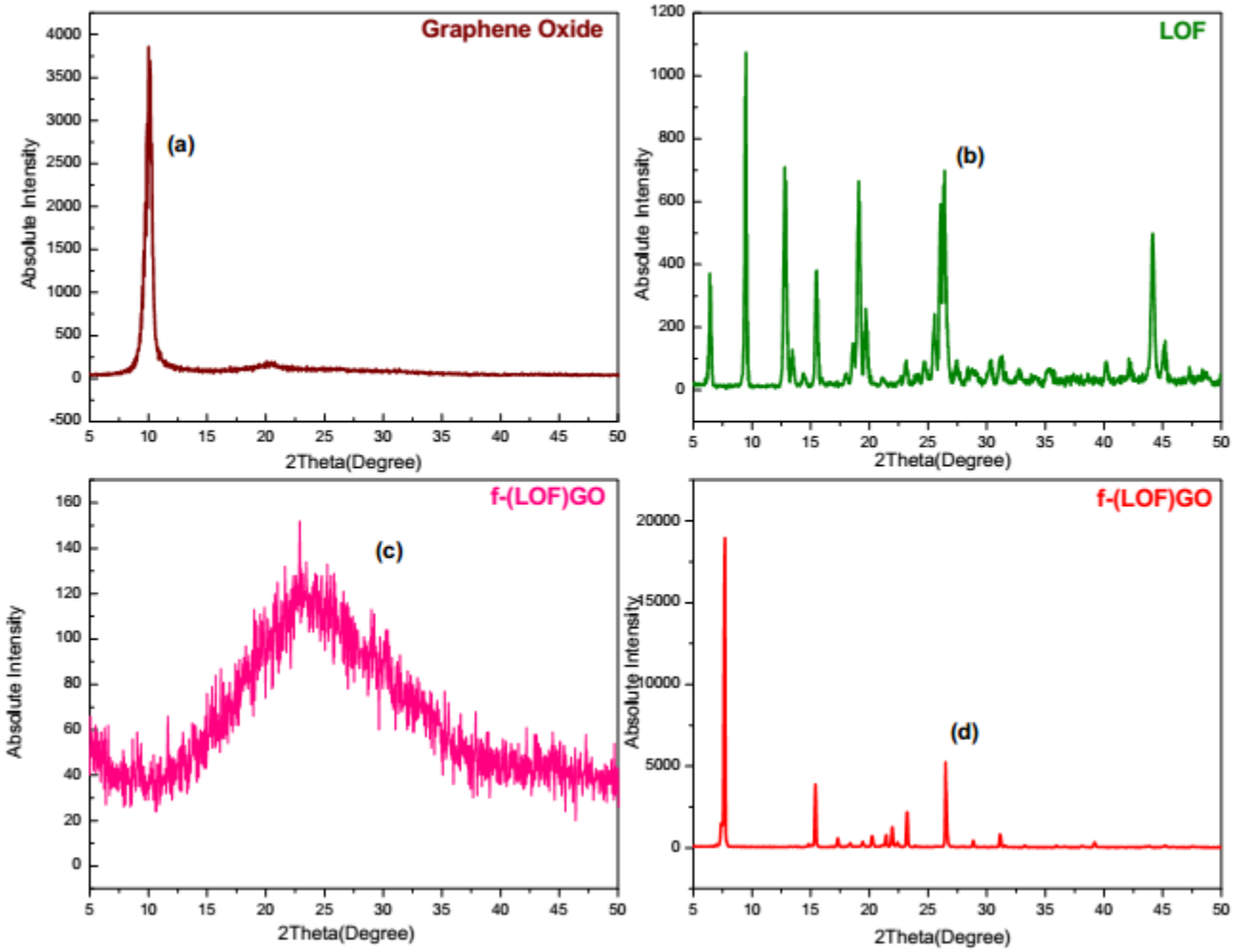


**Figure 6.** XRD patterns of (a) Graphene oxide (b) LOF (c) *f*-(LOF)GO vacuum dried (d) *f*-(LOF)GO drop casted

The interplanar distance for carbon layers was found to be increased from 3.4 Å to 8.7 Å. This increase in the "*d*" for GO has been attributed to the attachment of oxide functional groups to the graphite basal plane during oxidation reaction [7]. The most intense peak for graphite at 2 θ = 26.45$^o$ (corresponding to a *d*-spacing of 3.4 Å) is absent in this XRD pattern of GO sample which shows successful formation of GO. The crystalline structure of LOF was characterized by X-ray diffractogram as shown in Figure 6(b), that was in accordance with the reported literature [34]. After the functionalization reaction, when the coupled product was drop casted on the glass slide without removing excess LOF and diffraction pattern was obtained, the XRD pattern in Figure 6(d) contains some peaks of LOF along with the shift in the characteristic peak of GO from 10.5$^0$ to 26.5$^0$. After recovering graphene through solution processing and vacuum drying a broader diffraction peak was observed at 24$^0$ in Figure 6(c), which is attributed to reduction of "GO" and associated with large variation in the crystal size. This result is in agreement with the previous results [35-37]. This XRD profile clearly indicates coupling as well as the reduction of "GO". In this experiment functionalization of graphene along with its complete reduction was achieved which is evident from the absence of the 10.5$^0$ peak which is associated with the graphene oxide [7].

### *3.5. Electrochemical analysis*

CV measurement, an electrochemical method, is widely used to understand the electrochemical behavior of the functionalized GO [13]. The electrochemical behavior of the electrochemical cell fabricated with GO and *f*-(LOF)GO was analyzed in 1M $Na_2SO_4$ solution in a two electrode configuration test cell.

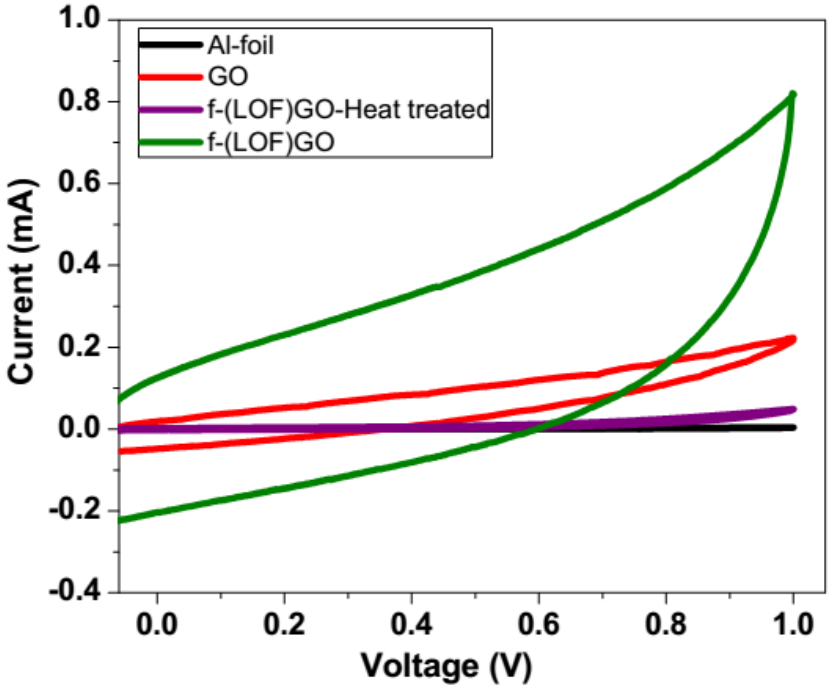


**Figure 7.** Cyclic voltammograms for Al-foil, GO and *f*-(LOF) GO and heat treated *f*-(LOF) GO at scan rate of 100 mV/s

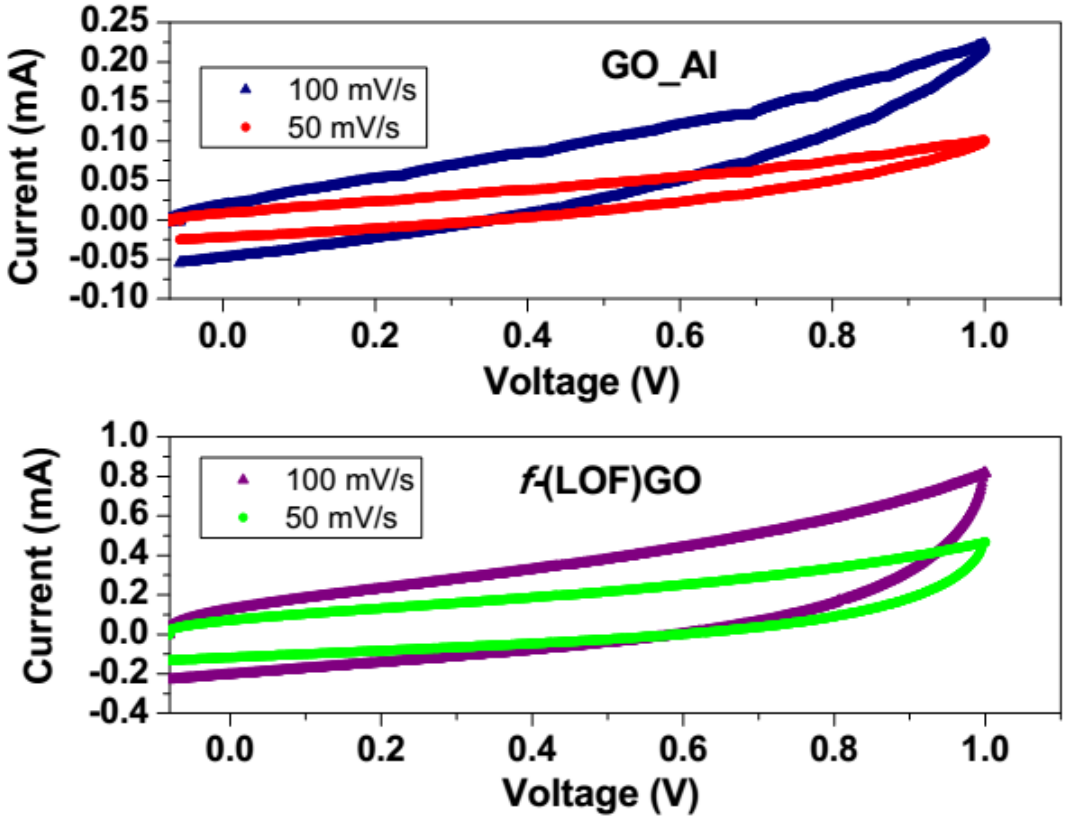


**Figure 8.** Cyclic voltammogram for GO and *f*-(LOF) GO at different scan rates

The electrochemical performances of Al and GO-Al have been investigated and reported earlier by Ban *et. al.* [18]. The CV curves of Al and GO-Al were used as a control and electrochemical behavior of *f*-(LOF)GO was investigated through cyclic voltammetery. CV curves exhibit quasi-rectangular shape without the presence of Faradic peaks which suggests the presence of double layer capacitance. Cyclic voltammetery curves in Figure 7 show that *f*-(LOF)GO coated on Al-foil has larger value of current as compared to the pristine GO coated on Al-foil. However the supercapacitive electrode, coated with *f*-(LOF)GO and heat treated at 200$^{o}$C in a glove box under N2 at 200$^{o}$C, displays current even lower than the pristine GO. This decrease in the current is due to the fact that the coating of the functionalized graphene on Al-foil was cracked upon heating and its electrical contact with Al-foil (current collector) was destroyed as evidenced by the SEM micrograph (Figure 5d). Capacitance for GO and *f*-(LOF)GO was determined by the division of current(mA) with scan rate(mV/s) of the CV curves, C=I/(dV/dt) [38]. CV studies were also performed from -0.1 mV to +1 mV at different scan rates. Figure 8 depicts the effect of voltage scan rate on the electrode currents of both GO and functionalized GO. At both scan rates shape of the CV curve is nearly same without any apparent distortion which illustrates admirable electronic and ionic transport inside the supercapacitor electrode material [39]. The capacitance of *f*-(LOF)GO_Al is 1.9mF while the capacitance of GO-Al and Al-foil is 0.522mF and 0.0119mF respectively. Since capacitance of the *f*-(LOF) GO_Al was four times the capacitance of GO which indicates the functionalization has significantly enhanced the electrochemical performance of GO. Moreover a higher current with increasing voltage scan rate justifies very good capacitive response for these electrodes**.**

## 4. CONCLUSION

In summary, the *f*-(LOF) GO has been successfully synthesized by esterification reaction which leads to functionalization and in-situ reduction process without using any toxic reducing agent. The coupled product was characterized by UV-Vis spectroscopy, XRD, FTIR, SEM and EDX to investigate the structure, morphology, functionalization and composition. All the results established the reduction as well as formation of *f*-(LOF) GO. Cyclic voltammetery shows large current and greater area for *f*-(LOF) GO as compared to GO. Capacitance of the *f*-(LOF) GO-Al was found to be four times the capacitance of GO which indicates the functionalization has significantly enhanced the electrochemical performance of GO.

ACKNOWLEDGEMENT
Z.H. gratefully acknowledges support from Prof. Dr. M. Mujahid, SCME – NUST for CV measurement through BioLogic VSP System purchased under NRPU project No. 20-1603/R&D/09/2236 funded by the Higher Commission (HEC) of Pakistan..

## References

1. A.K. Geim, K.S. Novoselov, *Nature materials*, 6 (2007) 183-191.
2. D.A. Brownson, D.K. Kampouris, C.E. Banks, *Journal of Power Sources*, 196 (2011) 4873-4885.
3. O.C. Compton, S.T. Nguyen, *Small*, 6 (2010) 711-723.
4. Y. Zhu, S. Murali, W. Cai, X. Li, J.W. Suk, J.R. Potts, R.S. Ruoff, *Advanced Materials*, 22 (2010) 3906-3924.
5. H. Kim, Y. Miura, C.W. Macosko, *Chemistry of Materials*, 22 (2010) 3441-3450.
6. K.S. Novoselov, A.K. Geim, S. Morozov, D. Jiang, Y. Zhang, S.a. Dubonos, I. Grigorieva, A. Firsov, *Science*, 306 (2004) 666-669.
7. N.M. Huang, H. Lim, C. Chia, M. Yarmo, M. Muhamad, *International journal of nanomedicine*, 6 (2011) 3443.
8. P. Zhu, M. Shen, S. Xiao, D. Zhang, *Physica B: Condensed Matte*r, 406 (2011) 498-502.
9. S. Stankovich, R.D. Piner, X. Chen, N. Wu, S.T. Nguyen, R.S. Ruoff, *Journal of Materials Chemistry*, 16 (2006) 155-158.
10. A. Furst, R.C. Berlo, S. Hooton, *Chemical Reviews*, 65 (1965) 51-68.
11. T. Kuila, S. Bose, A.K. Mishra, P. Khanra, N.H. Kim, J.H. Lee, *Progress in Materials Science*, 57 (2012) 1061-1105.
12. M. Fang, K. Wang, H. Lu, Y. Yang, S. Nutt, J*ournal of Materials Chemistry*, 20 (2010) 1982-1992.
13. Y. Hu and X. Sun, Advances in Graphene Science (Chapter 7), Dr. M. Aliofkhazraei (Ed.), ISBN: 978-953-51-1182-5, InTech, 2013.
14. J. Kauppila, P. Kunnas, P. Damlin, A. Viinikanoja, C. Kvarnström, *Electrochimica Acta*, 89 (2013) 84-89.
15. H.J. Salavagione, M.A. Gómez, G. Martínez, *Macromolecules*, 42 (2009) 6331-6334.
16. S. Pei, H.-M. Cheng, *Carbon*, 50 (2012) 3210-3228.
17. J. Zhang, H. Yang, G. Shen, P. Cheng, J. Zhang, S. Guo, *Chemical Communications*, 46 (2010) 1112-1114.
18. F. Ban, S.R. Majid, N.M. Huang, H.N. Lim, *International Journal of Electrochemical Science*, 7 (2012).

19. D.C. Marcano, D.V. Kosynkin, J.M. Berlin, A. Sinitskii, Z. Sun, A. Slesarev, L.B. Alemany, W. Lu, J.M. Tour, *ACS Nano*, 4 (2010) 4806-4814.
20. J. Shang, L. Ma, J. Li, W. Ai, T. Yu, G.G. Gurzadyan, *Scientific reports*, 2 (2012).
21. M. Cicuéndez, I. Izquierdo-Barba, M.T. Portolés, M. Vallet-Regí, *European Journal of Pharmaceutics and Biopharmaceutics*, 84 (2013) 115-124.
22. F.T. Thema, M.J. Moloto, E.D. Dikio, N.N. Nyangiwe, L. Kotsedi, M. Maaza, M. Khenfouch, *Journal of Chemistry*, 2013 (2013) 6.
23. Y. Xu, H. Bai, G. Lu, C. Li, G. Shi, *Journal of the American Chemical Society*, 130 (2008) 5856-5857.
24. Y. Li, X. Huang, Y. Li, Y. Xu, Y. Wang, E. Zhu, X. Duan, Y. Huang, *Scientific reports*, 3 (2013).
25. Z. Liu, X. Duan, X. Zhou, G. Qian, J. Zhou, W. Yuan, *Industrial & Engineering Chemistry Research*, 53 (2013) 253-258.
26. D. Liu, G. Huang, Y. Yu, Y. He, H. Zhang, H. Cui, *Chemical Communications*, 49 (2013) 9794-9796.
27. P. Karthika, N. Rajalakshmi, K.S. Dhathathreyan, *Soft Nanoscience Letters*, 2 (2012), 59-66.
28. M.S. Diallo, Nanotechnology for Sustainable Development, Springer, 2014.
29. M. Reddy, S. Eswaraiah, K. Reddy, P. Prakash, in, Google Patents, 2004.
30. A.K. Mishra, S. Ramaprabhu, *The Journal of Physical Chemistr*y C, 115 (2011) 14006-14013.
31. I. Roy, D. Rana, G. Sarkar, A. Bhattacharyya, N.R. Saha, S. Mondal, S. Pattanayak, S. Chattopadhyay, D. Chattopadhyay, *RSC Advance*s, 5 (2015) 25357-25364.
32. J. Molina, A. Zille, J. Fernández, A.P. Souto, J. Bonastre, F. Cases, *Synthetic Metals*, 204 (2015) 110-121.
33. B.S. Murty, P. Shankar, B. Raj, B. Rath, J. Murday, Textbook of nanoscience and nanotechnology, Springer Science & Business Media, 2013.
34. M. Reddy, S. Eswaraiah, K. Reddy, P. Prakash, in, Google Patents, 2004.
35. A.V. Murugan, T. Muraliganth, A. Manthiram, *Chemistry of Materials*, 21 (2009) 5004-5006.
36. X. Xu, T. Wu, F. Xia, Y. Li, C. Zhang, L. Zhang, M. Chen, X. Li, L. Zhang, Y. Liu, J. Gao, *Journal of Power Sources*, 266 (2014) 282-290.
37. Z. Bo, X. Shuai, S. Mao, H. Yang, J. Qian, J. Chen, J. Yan, K. Cen, *Scientific Reports*, 4 (2014) 4684.
38. M.D. Stoller, S. Park, Y. Zhu, J. An, R.S. Ruoff, *Nano Letters*, 8 (2008) 3498-3502.
39. S. Biswas, L.T. Drzal, *Chemistry of Materials*, 22 (2010) 5667-5671.